

Effective Photoimmunotherapy of Murine Colon Carcinoma Induced by the Combination of Photodynamic Therapy and Dendritic Cells

Ahmad Jalili,¹ Marcin Makowski,¹
Tomasz Świtaj,¹ Dominika Nowis,¹
Grzegorz M. Wilczyński,³ Ewa Wilczek,³
Magdalena Chorąży-Massalska,⁴
Anna Radzikowska,⁴ Włodzimierz Maśliński,⁴
Łukasz Biały,² Jacek Sieńko,⁵ Aleksander Sieroń,⁶
Mariusz Adamek,⁶ Grzegorz Basak,¹
Paweł Mróz,¹ Ireneusz W. Krasnołębski,⁷
Marek Jakóbisziak,¹ Jakub Gołąb¹

Departments of ¹Immunology, ²Histology and Embryology, and ³Pathology, Center of Biostructure Research, The Medical University of Warsaw, Warsaw; ⁴Department of Pathophysiology and Immunology, Institute of Rheumatology, Warsaw, ⁵II Department and Clinic of Obstetrics and Gynecology, The Medical University of Warsaw, Warsaw; ⁶Center for Laser Diagnostics and Therapy, Chair and Clinic of Internal Diseases and Physical Medicine, Silesian Medical University, Bytom; and ⁷Department of General, Gastrointestinal Surgery and Nutrition, The Medical University of Warsaw, Warsaw, Poland

ABSTRACT

Purpose: The unique mechanism of tumor destruction by photodynamic therapy (PDT), resulting from apoptotic and necrotic killing of tumor cells accompanied by local inflammatory reaction and induction of heat shock proteins (HSPs), prompted us to investigate the antitumor effectiveness of the combination of PDT with administration of immature dendritic cells (DCs).

Experimental Design: Confocal microscopy and Western blotting were used to investigate the influence of PDT on

the induction of apoptosis and expression of HSP expression in C-26 cells. Confocal microscopy and flow cytometry studies were used to examine phagocytosis of PDT-treated C-26 cells by DCs. Secretion of interleukin (IL)-12 was measured with ELISA. Cytotoxic activity of lymph node cells was evaluated in a standard ⁵¹Cr-release assay. The antitumor effectiveness of PDT in combination with administration of DCs was investigated in *in vivo* model.

Results: PDT treatment resulted in the induction of apoptotic and necrotic cell death and expression of HSP27, HSP60, HSP72/73, HSP90, HO-1, and GRP78 in C-26 cells. Immature DCs cocultured with PDT-treated C-26 cells efficiently engulfed killed tumor cells, acquired functional features of maturation, and produced substantial amounts of IL-12. Inoculation of immature DCs into the PDT-treated tumors resulted in effective homing to regional and peripheral lymph nodes and stimulation of cytotoxic activity of T and natural killer cells. The combination treatment with PDT and administration of DCs produced effective antitumor response.

Conclusions: The feasibility and antitumor effectiveness demonstrated in these studies suggest that treatment protocols involving the administration of immature DCs in combination with PDT may have clinical potential.

INTRODUCTION

Photodynamic therapy (PDT) is a promising treatment of various malignant and nonmalignant disorders. It involves systemic administration of a photosensitizer that preferentially accumulates in transformed cells followed by an illumination of the tumor with a monochromatic and collimated beam of laser light (1). In the presence of oxygen, the laser light activates the photosensitizer and initiates a complex photochemical reaction that generates cytotoxic intermediates (2). The mechanism of higher photosensitizer retention in the tumor as compared with normal tissues has not been fully elucidated but probably results from the binding of Photofrin to low-density lipoproteins the receptors for which are expressed on tumor cells, better photosensitizer internalization at low pH, impaired lymphatic drainage, or a combination of these factors. Photofrin-based PDT has been approved by the FDA for treatment of early and late endobronchial non-small cell lung cancer in patients for whom surgery and radiotherapy are contraindicated, and for palliative treatment of advanced esophageal cancer (1, 3). Approval is pending for early-stage esophageal cancer in conjunction with Barrett's esophagus. Another photosensitizer, temoporfin, has been approved in the European Union for the palliative treatment of patients with advanced head and neck cancer, and 5-aminolevulinic acid-based PDT is approved for the treatment of skin and head and neck cancers in many countries of the

Received 2/25/04; revised 4/8/04; accepted 4/12/04.

Grant support: Grants 1M19/M2, 1M19/NK and 1M19/W1 from the Medical University of Warsaw, Poland; Grants 4 P05A 025 18 and PBZ-KBN-091/P05/54 from the State Committee for Scientific Research; a grant from the Foundation for Polish Science

The costs of publication of this article were defrayed in part by the payment of page charges. This article must therefore be hereby marked *advertisement* in accordance with 18 U.S.C. Section 1734 solely to indicate this fact.

Note: A. Jalili is a student of the Postgraduate School of Molecular Medicine in Warsaw and a recipient of the Scholarship from the Leopold Kronenberg Foundation, and is currently at Universitätsklinik für Dermatologie, Abteilung für Immundefektologie und Infektiose Hautkrankheiten, Allgemeines Krankenhaus der Stadt Wien, Vienna, Austria; Dominika Nowis is the recipient of the Foundation for Polish Science Award.

Requests for reprints: Jakub Gołąb, Department of Immunology, Center of Biostructure Research, The Medical University of Warsaw, Chałubińskiego 5, 02-004 Warsaw, Poland. Phone/Fax: 4822-622-6306; E-mail: jgolab@ib.amwaw.edu.pl.

European Union. At least five other photosensitizers are in various stages of clinical trials.

Tumor destruction after PDT results from direct cytotoxic effects toward tumor cells and vascular damage, as well as from the induction of local inflammatory response (1, 4, 5). The relative contribution of all of these mechanisms is difficult to establish, but it seems that all of them are necessary for the successful outcome of the treatment. Extensive preclinical studies are being held to optimize each of these mechanisms for the most effective curative effects of PDT.

Accumulating evidence indicates that effective control over the PDT-treated tumors is exerted by the immune system. PDT is less effective in immunodeficient or in immune cells-depleted animals (6). Moreover, several immune-stimulating cytokines or immunomodulators and adoptive transfer of immune cells have been shown to potentiate the antitumor effectiveness of PDT (7–11). In some tumor models, PDT is even capable of controlling distant disease (12); but in others, this treatment was shown to increase the number of lung metastases (13). This latter observation should be kept in mind during translating the results of animal studies into a clinical setting. Despite the potential involvement of the immune system in the antitumor effects of PDT, this treatment modality is usually inefficient in the complete eradication and long-term control over disseminated tumors. Therefore, approaches that would exploit the effects of PDT for the induction of an effective systemic immunity are intensively being pursued.

Dendritic cells (DCs) are the professional antigen-presenting cells and the most effective inducers of adaptive immunity (14). These cells efficiently acquire antigens from apoptotic and necrotic tumor cells (15). This process is restricted to the immature stage of development, when DCs are effectively acquiring antigens but express low levels of MHC and costimulatory molecules. Immature DCs present antigens quite inefficiently. Additional signals, often referred to as danger signals, induce maturation, which transforms DCs into effective antigen-presenting cells that migrate to regional lymph nodes for the activation of T lymphocytes (16). Whereas a number of microbial products have been shown to provide maturation signals for immature DCs, it has not yet been unequivocally resolved what are the danger signals necessary for the effective stimulation of DCs interacting with dying tumor cells. Accumulating evidence indicates that some heat shock proteins (HSPs) might play this role (17–19).

The present study builds on the observations that PDT induces both necrotic and apoptotic death of tumor cells accompanied by oxidative stress and induction of HSPs. Therefore, PDT creates a unique environment that provides tumor antigens accompanied by “danger” signals that could trigger maturation signals for DCs. The aim of these studies was, therefore, to check whether the combination treatment with PDT followed by the administration of immature DCs could induce an effective antitumor immunity.

MATERIALS AND METHODS

Mice. BALB/c mice, 8–12 weeks of age, were used in the experiments. Breeding pairs were obtained from the Institute of Oncology (Warsaw, Poland). All of the experiments with

animals were performed in accordance with the guidelines approved by the Ethical Committee of the Medical University of Warsaw.

Reagents. Photofrin was a generous gift of QLT Photo-Therapeutics, Inc. (Vancouver, BC, Canada). A vital nonphoto-toxic fluorescent dye, 5,6-carboxyfluorescein diacetate succinimidyl ester (CFSE), was purchased from Molecular Probes (Leiden, the Netherlands).

Tumors. Murine Colon-26 (C-26, a poorly differentiated, immunogenic colon adenocarcinoma cell line) cells were obtained from Professor Czesław Radzikowski (Institute of Immunology and Experimental Medicine, Wrocław, Poland). Cells were cultured in RPMI 1640 (Invitrogen, Carlsbad, CA), supplemented with 10% heat-inactivated FCS, antibiotics, 50 μ M 2-mercaptoethanol, and 2 mM L-glutamine (all from Invitrogen), hereafter referred to as culture medium.

Isolation and Culture of Bone Marrow DCs. DCs were isolated and cultured according to the method of Inaba *et al.* (20) and as described previously (21). Briefly, DCs were obtained from bone marrow precursors by flushing femur, tibia, and humerus bones of 8–10-week-old BALB/c mice with cold PBS. RBCs were lysed using ammonium chloride. Cells (1×10^7 cells/5 ml/well) were then cultured in 6-well plates (Nunc, Roskilde, Denmark) in culture medium, and 10 ng/ml granulocyte macrophage colony-stimulating factor (GM-CSF; Pepro-Tech, EC, Ltd, London, United Kingdom). On the 2nd day, the culture medium was removed and fresh medium containing 10 ng/ml GM-CSF (PeproTech) and 5 ng/ml interleukin (IL)-4 (PeproTech) was added. The procedure was followed by replacing 75% of medium with a fresh one containing 10 ng/ml GM-CSF and 5 ng/ml IL-4 on day 4. Loosely adherent cells were replated on day 6 into new 6-well plates at a concentration of 5×10^6 cells/5 ml/well in culture medium containing 10 ng/ml GM-CSF and 5 ng/ml IL-4. On day 8, the cells, collected by gently scraping (Cell Scraper, 23 cm; Nunc) the wells, were used for the experiments.

Histopathology and TUNEL Staining. Individual C-26 tumors were excised and snap-frozen 24 h after PDT (10 mg/kg Photofrin; 90 J/cm² light dose). Several cryostat sections, 10 μ m thick, were cut from each tumor. Some sections were stained with H&E routinely, the other sections underwent terminal deoxynucleotidyl transferase-mediated nick end labeling (TUNEL) staining.

DNA fragmentation was detected by terminal deoxynucleotidyl transferase-based, *in situ* cell death detection kit (TUNEL; Boehringer Mannheim, Mannheim, Germany). The procedure was performed according to the manufacturer's instructions.

Western Blotting and Confocal Laser Scanning Microscopy. For Western blotting and immunofluorescence studies, C-26 cells were cultured with 5 μ g/ml Photofrin for 24 h before illumination. After a washing with PBS, the cells were illuminated with a 50-W sodium lamp (Philips) with a light filtered through a red filter to a final dose of 4.5 kJ/m², as described previously (22). After 4 h of culture in the fresh medium, the cells were washed with PBS and were lysed with radioimmunoprecipitation assay (RIPA) buffer (Tris base 50 mM, NaCl 150 mM, NP40 1%, sodium deoxycholate 0.25%, EDTA 1 mM) with protease inhibitors cocktail (Roche Diagnostics, Mannheim, Germany). Protein concentration was measured with the use of

BCA protein assay (Pierce, Rockford, IL). Equal amounts of proteins were separated on 10% SDS-polyacrylamide gel, transferred onto polyvinylidene difluoride membranes, blocked with TBST [Tris-buffered saline (pH 7.4), 0.05% Tween 20] with 5% nonfat milk and 5% fetal bovine serum. The following antibodies were used for the 2-h incubation: mouse monoclonal anti-tubulin, goat polyclonal anti-HSP60, mouse monoclonal anti-HSP70, rabbit polyclonal anti-HSP90, goat polyclonal anti-HO-1, goat polyclonal anti-GRP78, goat polyclonal anti-GRP94, mouse monoclonal anti-HSP72/73, goat polyclonal anti-HSP27 at 1:1000 (all from Santa Cruz Biotechnology, Inc., Santa Cruz, CA). After extensive washing with TBST, the membranes were incubated for 45 min in corresponding alkaline phosphatase-coupled secondary antibodies (Jackson Immuno Research Inc. West Grove, PA). The color reaction was developed using NBT (*p*-nitro-blue tetrazolium chloride) and BCIP (5-bromo-4-chloro-3-indolyl-phosphate; Sigma). The immunofluorescent-microscopic studies were performed in cytospin preparations of the cells collected at 4 h after PDT. The specimens were air-dried, fixed in acetone (at -20°C), and then incubated in 5% normal donkey serum (Jackson Immunoresearch) in PBS for 1 h at room temperature to reduce nonspecific binding. The primary antibodies (the same as in Western blot studies) were applied overnight at 4°C , diluted 1:500 in 5% normal donkey serum in PBS, except for the anti-HSP72/73 antibody, which was used at the dilution of 1:100. Secondary detection reagents (all from Jackson Immunoresearch) were: donkey antirabbit or donkey antimouse antibodies conjugated to Cy3 fluorochrome, or biotinylated donkey antigoat antibody followed by streptavidin-Cy3. Cell nuclei were counterstained with Hoechst 33342 (Molecular Probes). After being mounted in Vectashield medium (Vector) and coverslipped, the specimens were examined under the Leica TCS SP2 laser confocal microscope (Leica, Mannheim, Germany), using the HeNe 543 nm, and MaiTai IR femto (double-photon operating at 780 nm) lasers, for Cy3 and Hoechst 33342 excitation respectively. The image-stacks of consecutive focal planes were collected with 0.5- μm z-interval, in 1024×1024 pixel format, using Plan Apo 63 \times oil, NA 1.32 objective, at no zoom. Subsequently, maximum intensity projections (extended focus images) were calculated from each fluorescence channel of the image stack and were stored as RGB (red-green-blue) images together with original image stacks. Special care was undertaken so as to keep the same instrument setting and operation-conditions while scanning control and PDT-treated samples.

Flow Cytometry. C-26 cells were stained with 5 μM CFSE for 5 min., were washed three times with PBS containing 5% fetal bovine serum, and were incubated with Photofrin (5 $\mu\text{g}/\text{ml}$) for 24 h. After illumination with a laser light ($10 \text{ kJ}/\text{m}^2$), the cells were incubated for 4 h at 37°C and 5% CO_2 . Then, immature bone marrow-derived DCs (1×10^5) were added in a volume of 100 μl and cocultured with PDT-treated C-26 cells for another 4 h. The cells were then collected and washed three times in PBS. Surface expression of MHC class II molecules was determined by incubating the cells with R-phycoerythrin (R-PE)-conjugated rat antimouse I-A/I-E monoclonal antibody against MHC class II antigen (PharMingen, San Diego, CA). After a 30-min incubation at 4°C , the cells were washed three times in PBS containing 2% heat-inactivated fetal bovine serum

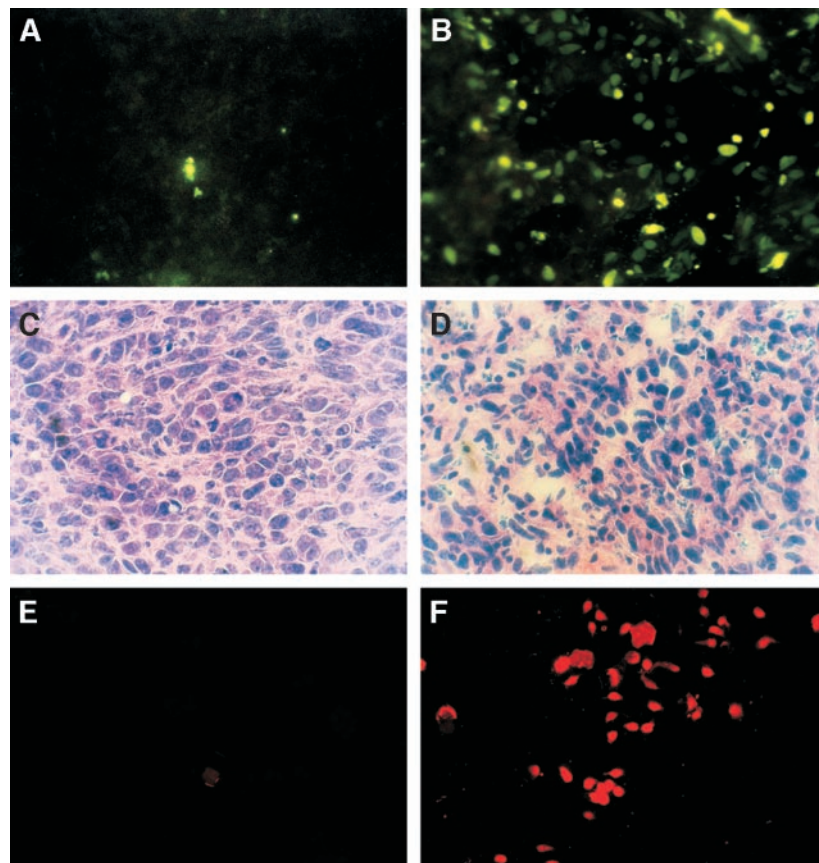
and 0.1% sodium azide and were fixed with PBS containing 1% paraformaldehyde (Polysciences, Warrington, PA). A total of 10,000 cells were analyzed using a FACScan (Becton Dickinson Immunocytometry, San Jose, CA).

Confocal Laser Scanning Microscopy for Coculture Experiments. C-26 cells were stained with CFSE and were incubated with Photofrin (5 $\mu\text{g}/\text{ml}$) for 24 h. After illumination with a laser light ($10 \text{ kJ}/\text{m}^2$) the cells were incubated for 4 h at 37°C and 5% CO_2 . Then, immature bone marrow-derived DCs (1×10^5) were added in a volume of 100 μl and cocultured with PDT-treated C-26 cells for another 4 h. The coculture was subsequently incubated with R-PE-conjugated rat antimouse I-A/I-E monoclonal antibody against MHC class II antigen (PharMingen; 1 h on ice), plated into a 16-well chamber slides (Nunc), and kept at 37°C until the majority of the cells attached to the glass surface (about 90 min). Then, the cells were fixed in 2% paraformaldehyde in PBS, rinsed in PBS, and (after disassembling the chamber-slide), mounted in Vectashield medium (Vector) and coverslipped. The specimens were examined under the Leica TCS SP2 laser confocal microscope (Leica), using the 488-nm line of the Argon laser and the 543-nm line of the HeNe laser, for CFSE and phycoerythrin excitation, respectively. The detection settings were adjusted so as to prevent any appreciable cross-talk between the fluorochromes. Along the z-axis, usually 20–30 thin optical sections with a z-step of 0.5 μm were scanned in a 1024×1024 pixel format. Images were taken with a Plan Apo 63 \times oil, NA 1.4 objective lens at various zoom factors. Subsequently, maximum intensity projections (extended focus images) were calculated from each fluorescence channel of the image stack and stored as RGB (red-green-blue) images together with original image stacks. Further image processing and two-dimensional deconvolution was performed with the use of AutoDeblur/Autovisualize 9.1 software (AutoQuant, Inc., Watervliet, NY).

Determination of Cytokine Concentrations. IL-12p40 and tumor necrosis factor (TNF) concentrations in culture supernatants were determined by commercially available ELISA kits (R&D Systems, Wiesbaden-Nordenstadt, Germany) according to the instructions of the manufacturer.

Chromium (^{51}Cr) Release Assay. Cytotoxic activity of lymph node cells and splenocytes from mice treated with PDT and/or DCs (for details, see the following section) was tested in a standard (^{51}Cr) release assay, as described previously (23). Lymph nodes and spleens were harvested and RBC-depleted single-cell suspensions were generated. In some cultures, recombinant IL-2 (Proleukin; specific activity of 18×10^6 units/ml) at 20 units/ml was added for 72 h. To deplete specific lymphocyte subsets, we used a magnetic cell-separation system (MACS; Miltenyi-Biotec, Bergisch Gladbach, Germany). Removal of CD8^+ and natural killer (NK) cells from splenocyte suspension was performed by passing magnetically labeled cells (with anti- CD8a and anti-NK MicroBeads) through a magnetic cell separator, according to the manufacturer's protocol. Finally, 100- μl aliquots of cells were added to ^{51}Cr -labeled C-26 cells. The cells were incubated either for 4 h or 18 h, the supernatants were collected, and the radioactivity of the ^{51}Cr released from target cells was measured in a gamma counter (Wallac, Gaithersburg, MD). Maximum ^{51}Cr release was determined in target cells treated with Triton X-100 at final concentration of 0.5%.

Fig. 1 Histopathological analysis and terminal deoxynucleotidyl transferase-mediated nick end labeling (TUNEL) staining of C-26 tumors treated with photodynamic therapy (PDT) *in vitro* and *in vivo*. Tumors were obtained from controls (A, C) and PDT-treated mice (B, D) on day 8 after inoculation with C-26 cells and 24 h after illumination with laser light (10 mg/kg Photofrin, and a light dose of 90 J/cm²). The apoptotic DNA fragmentation was detected by terminal deoxynucleotidyl transferase-based, *in situ* cell death detection kit (TUNEL). There are only single apoptotic cells in tumors from control animals (A) and a significant induction of apoptosis in tumors treated with PDT (B). H&E staining was performed routinely. In the sections of control tumors (C) densely packed neoplastic cells form a uniform and solid tumor mass. After PDT (D), the tumor architecture is markedly disturbed, with multiple foci of necrosis and/or apoptosis, and with occasional granulocyte infiltrations. Similar apoptotic effects were observed after PDT *in vitro*, when C-26 cells were incubated with 5 μg/ml Photofrin and illuminated with laser light at 10 kJ/m². *In vitro* treatment of C-26 cells (controls in E) leads to extensive DNA fragmentation after PDT (F).



The cytotoxicity was estimated as a cell lysis % according to the formula: cell lysis % = [(experimental release – spontaneous release)/(maximum release – spontaneous release)] × 100.

Tumor Treatment and Monitoring. For *in vivo* experiments exponentially growing C-26 cells were harvested, resuspended in PBS at a concentration of $2 \times 10^5/20 \mu\text{l}$ of PBS and were injected into the footpad of the right hind limb of experimental mice. Tumor cell viability measured by trypan blue exclusion was always above 95%. Photofrin was administered i.p. at a dose of 10 mg/kg, 24 h before illumination with 630-nm light (day 6 after inoculation with tumor cells). Control mice received 5% dextrose. The light source was a He-Ne ion laser (LaserProject 2000, Warsaw, Poland). The light was delivered to tumors on day 7 after inoculation with tumor cells using a fiberoptic light delivery system. The power density at the illumination area, which encompassed the tumor and 1–1.5 mm of the surrounding skin, was $\sim 80 \text{ mW/cm}^2$. The total light dose delivered to the tumors was 90 J/cm^2 . During the light treatment, mice were anesthetized with ketamine (87 mg/kg) and xylazine (13 mg/kg) and were restrained in a specially designed holder. On day 6 of the experiment, all of the mice were inoculated with 1×10^5 C-26 cell in the left (contralateral) hind limb. DCs (1×10^6) were injected into tumors growing in right hind limbs on days 7 (1 h after PDT) and 8. PBS was used as a control for DC injections. Local tumor growth was determined as described previously (24) by the formula: Tumor volume (mm^3) = (longer diameter) × (shorter diameter)²/2.

Statistical Analysis. Data were calculated using Microsoft Excel 98. Differences in *in vitro* cytotoxicity assays and in tumor volume were analyzed for significance by Student's *t* test. Significance was defined as a two-sided $P < 0.05$.

RESULTS

PDT-Treated Cells Undergo Both Apoptosis and Necrosis and Express HSPs. Numerous previous studies have shown that PDT can induce both necrosis and apoptosis in tumor cells. The relative contribution of these processes to the overall kill of tumor cells depends mainly on the photosensitizer concentration and/or the light dose. To validate these observations in our tumor model, we inoculated mice with 1×10^5 viable C-26 cells and then treated tumors with PDT (Photofrin was administered on day 6 after inoculation of tumor cells at a dose of 10 mg/kg, and the light was delivered on day 7 at a dose of 90 J/cm^2). We observed that, at these defined conditions, Photofrin-based PDT could induce apoptosis in C-26 cells (Fig. 1, A and B). H&E staining of the tumor specimens revealed that the PDT-treated tumors contained regions of necrosis (Fig. 1, C and D). The tumors of mice treated with PDT were edematous and painful (mice tried not to use the treated limbs), indicating that the treatment induced local inflammation typical for the necrosis but not for apoptosis. *In vitro* treatment of C-26 with PDT also induced apoptosis in tumor cells (Fig. 1E).

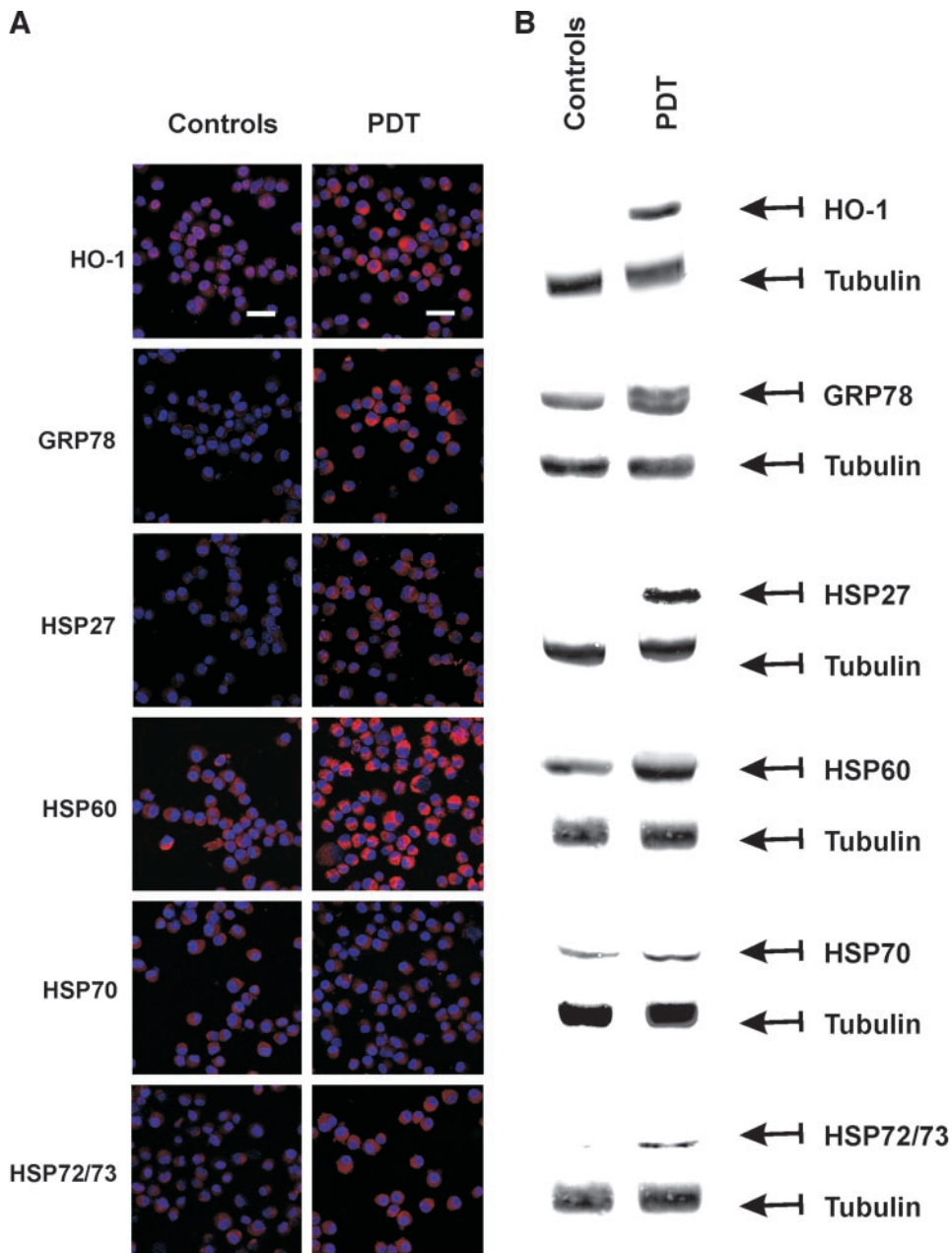


Fig. 2 Heat shock protein (HSP) expression in C-26 cells after photodynamic therapy (PDT) *in vitro*. C-26 cells were incubated with 5 $\mu\text{g}/\text{ml}$ Photofrin for 24 h before illumination with a laser light at a dose of 5 kJ/m^2 . *A*, after 4 h, the cells were stained with antibodies against HO-1, GRP78, HSP27, HSP60, HSP70, and HSP72/73. *B*, cell lysates were collected at 0 h and 4 h after PDT and were assayed for HSP expression and tubulin levels with Western blotting.

Because PDT causes an oxidative stress in treated tumor cells that leads to increased expression of several HSPs, we decided to investigate the influence of PDT on the expression of a panel of HSPs including those that were reported to influence the function of DCs. Confocal laser scanning microscopy studies performed with cells collected 4 h after PDT revealed that this treatment leads to a significant induction of HSP60, hem oxygenase 1 (HO-1, also referred to as HSP34), GRP78, and HSP90. *In vitro* treated C-26 cells also expressed slightly elevated levels of HSP27 and HSP72/73. No induction of HSP70 or GRP94 was observed (Fig. 2). Western blotting analysis confirmed these observations.

PDT-Treated C-26 Cells Can Be Endocytosed by Immature DCs Leading to Their Activation. To induce an effective immune response, DCs need first to ingest tumor-derived material before processing it and presenting to T cells. Therefore, we decided to investigate whether DCs are able of endocytosing PDT-damaged tumor cells or tumor cell fragments. C-26 cells were stained with CFSE, a fluorescent dye that gives a strong and stable green fluorescence. CFSE-labeled C-26 cells were incubated with Photofrin for 24 h and were exposed to laser light. Coculture of CFSE-labeled and PDT-treated C-26 cells (but not untreated C-26 controls) with DCs resulted in an efficient uptake of tumor cells and/or tumor cell

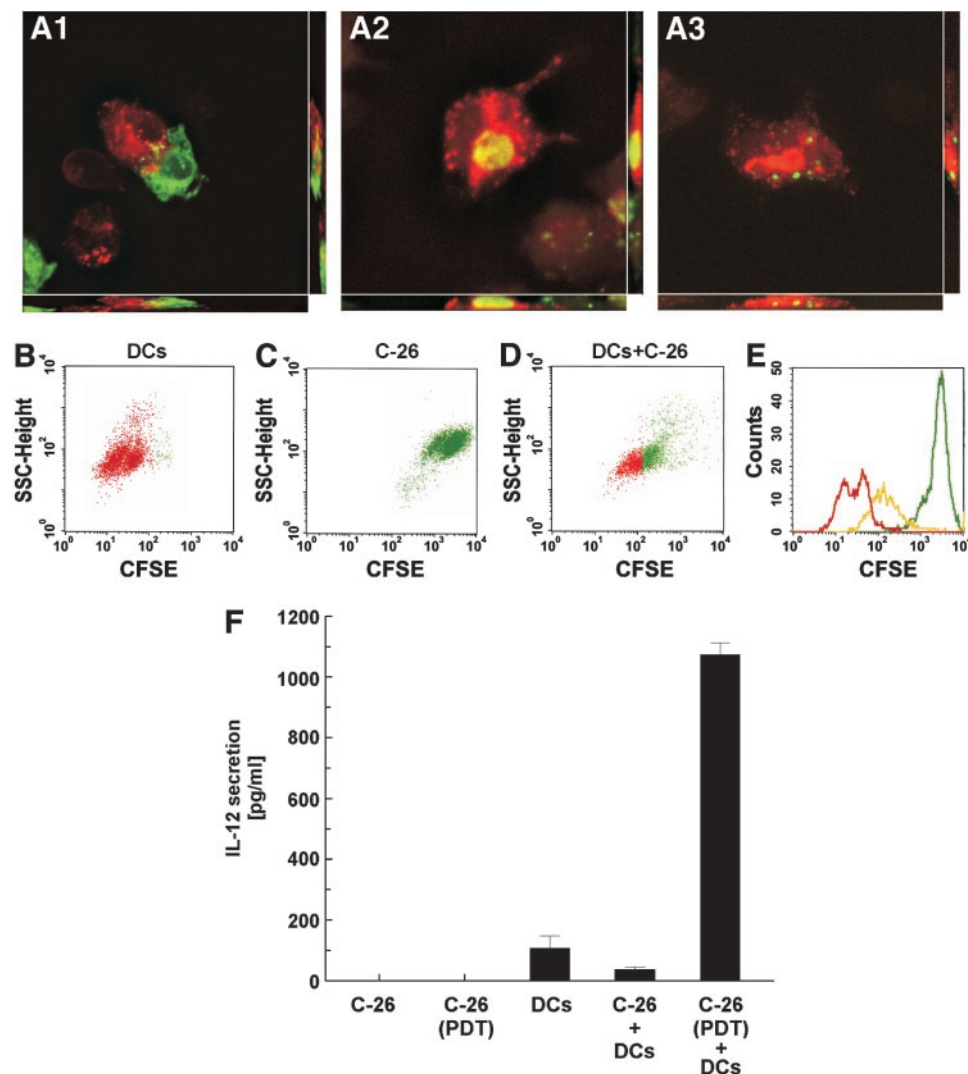


Fig. 3 Capture of photodynamic therapy (PDT)-treated C-26 cells by immature dendritic cells (DCs). C-26 cells were labeled with a fluorescent dye [5,6-carboxyfluorescein diacetate succinimidyl ester (CFSE)] before incubation with Photofrin ($5 \mu\text{g/ml}$) and illumination with laser light (10 kJ/m^2). DCs were added to PDT-treated C-26 cells 4 h after PDT and were incubated for another 4 h before staining with PE-conjugated antimouse I-A/I-E monoclonal antibody against MHC class II antigen. Confocal laser scanning microscopy in **A**, DCs (red) interacting with CFSE-labeled C-26 cells (green, **A1**) as well as fragments of C-26 cells ingested by DCs (**A2**, **A3**). **B** and **D**, dot-plots of cells showing CFSE fluorescence; these cells were gated for the expression of MHC class II molecules. **C**, CFSE-labeled C-26 cells. **E**, a histogram composition of cells in **B–D**, showing a relative CFSE fluorescence in DCs (red), DCs cocultured with CFSE-labeled C-26 cells (orange), and CFSE-labeled C-26 cells (green). **F**, the concentrations of interleukin 12 (IL-12) secreted by DCs cocultured with PDT-treated C-26 cells. C-26 cells were plated into wells of 96-well plates (2×10^4 /well) and were incubated for 24 h with Photofrin (5 mg/ml). After illumination with a laser light (10 kJ/m^2), the cells were incubated for 4 h at 37°C and 5% CO_2 . Then, immature bone marrow-derived DCs (1×10^5) were added and cocultured with PDT-treated C-26 cells for another 24 h. The concentrations of IL-12 were measured directly from culture supernatants. **B–E**, SSC, side scatter.

remnants, as demonstrated by confocal laser scanning microscopy (Fig. 3A–C). Some DCs were observed to interact directly with lethally damaged tumor cells [there were numerous blebs and vacuoles at the surface of tumor cell (green) shown in Fig. 3A1]. There were DCs that contained large (Fig. 3A2) as well as small (Fig. 3A3) fragments of C-26 cells. The flow cytometry analysis confirmed observations with confocal laser scanning microscopy. Whereas only 3% of DCs cocultured with control C-26 cells contained green fluorescence (Fig. 3B), 51% of such cells contained green fluorescence when cocultured with PDT-treated and CFSE-labeled C-26 cells (Fig. 3D).

The next question was whether DCs become functionally activated after interaction with PDT-treated C-26 cells. One of the most important secreted mediators of activated DCs is IL-12, a cytokine with potent antitumor activity and the ability to polarize T helper 1 cell (Th1)/Th2 response. Unstimulated DCs produced three times more IL-12 than did DCs cocultured with control C-26 cells ($107.93 \pm 33.33 \text{ pg/ml}$ and $37.38 \pm 7.74 \text{ pg/ml}$, respectively). Importantly, DCs cocultured with PDT-treated C-26 cells produced 10 times more IL-12 than did unstimulated controls ($1073.22 \pm 39.34 \text{ pg/ml}$; Fig. 3F). Altogether, the results of these studies unequivocally showed that

Table 1 Migration of CFSE-labeled DCs to lymph nodes.

Balb/c mice ($n = 9$) were inoculated with C-26 cells (1×10^5). Seven days later the tumors were treated with PDT (10 mg/kg Photofrin, and a light dose of 90 J/cm²). Immature CFSE-labeled DCs (1×10^6) were inoculated into untreated (control) tumors or into PDT-treated tumors and 24 h later lymph nodes were removed and the cell suspensions were analyzed for fluorescence using flow cytometry. The values refer to the median number (range) of CFSE-positive cells per lymph node.

Group	Regional lymph nodes	Peripheral lymph nodes
Control tumors	2250(1360–2860)	250(210–1350)
PDT-treated tumors	1120(570–3570)	640(510–2420)

CFSE, 5,6-carboxyfluorescein diacetate succinimidyl ester; DC, dendritic cell; PDT, photodynamic therapy.

DCs can interact with and efficiently endocytose PDT-treated tumor cells or tumor cell fragments and become functionally activated.

Intratumorally Injected Immature DCs Can Home to Lymph Nodes and Induce an Immune Response. In the next step we decided to investigate whether intratumorally (i.t.) injected DCs are able to reach local lymph nodes, where in appropriate environment they could present antigens to naive T cells. CFSE-labeled DCs were injected into control or PDT-treated C-26 tumors growing in BALB/c mice. After 24 h, the local (popliteal) as well as distant (cervical) lymph nodes were isolated, and cell suspensions were analyzed with flow cytometry. Of 1×10^6 DCs inoculated into untreated C-26 tumors, >0.2% managed to get into local and even less into distant lymph nodes (Table 1). Importantly, DCs injected into C-26 tumors at 1 h after PDT also migrated to the lymph nodes.

Although the number of DCs that must reach lymphatic tissue for an effective immune response is unknown, it was shown that i.v. administration of as few as 9×10^3 DCs pulsed with tumor peptides had a measurable antitumor effect (25). The antigen-loading capacity of DCs after *in vivo* PDT was not determined in this study. However, the finding of effective endocytosis of PDT-treated C-26 cells and the capacity to migrate to the lymph nodes warranted additional *in vivo* experiments aimed at verifying the potential of DCs to induce adaptive immune response in the therapeutic schedule that might be easily adopted for the combination treatment.

Seven days after treatment (PDT followed by inoculation of 1×10^6 DCs), regional lymph nodes and spleens were removed from mice, and the cytotoxic activity of the lymphocytes was measured in 4-h and 18-h cytotoxicity assays that measure, respectively, spontaneous cytotoxicity (attributed to NK cells) as well as specific cytotoxicity (attributed mainly to CD8⁺ T cells). Whereas there was no measurable stimulation of lymphocyte cytotoxicity in mice treated with PDT or DCs alone, inoculation of DCs into PDT-treated C-26 tumors growing in BALB/c mice resulted in a significant stimulation of lymph node cells' cytotoxicity toward tumor cells (Fig. 4, A and B). A brief expansion of lymph node cells with IL-2 resulted in the stimulation of spontaneous cytotoxicity in all of the treated groups of mice and a 2-fold increase in the cytotoxicity measured after an 18-h incubation (Fig. 4, C and D). Interestingly, administration of DCs alone led to a 5-fold (as compared with

controls) stimulation of cytotoxicity of spleen-derived lymphocytes (Fig. 4E). A comparable cytotoxic activity was found in spleen cells obtained from mice treated with a combination of PDT and DCs. Depletion studies revealed that the cytotoxic activity (measured only in spleen cells because of the paucity of lymph node cells for the depletion studies) can be attributed to both NK and CD8⁺ T cells (Fig. 4E). The culture supernatants of spleen lymphocytes from mice treated with DCs alone or in combination with PDT contained increased concentrations of TNF, a cytokine that is necessary for the induction of adaptive immunity and that is one of the mediators of NK and T-cell cytotoxicity (Fig. 4F).

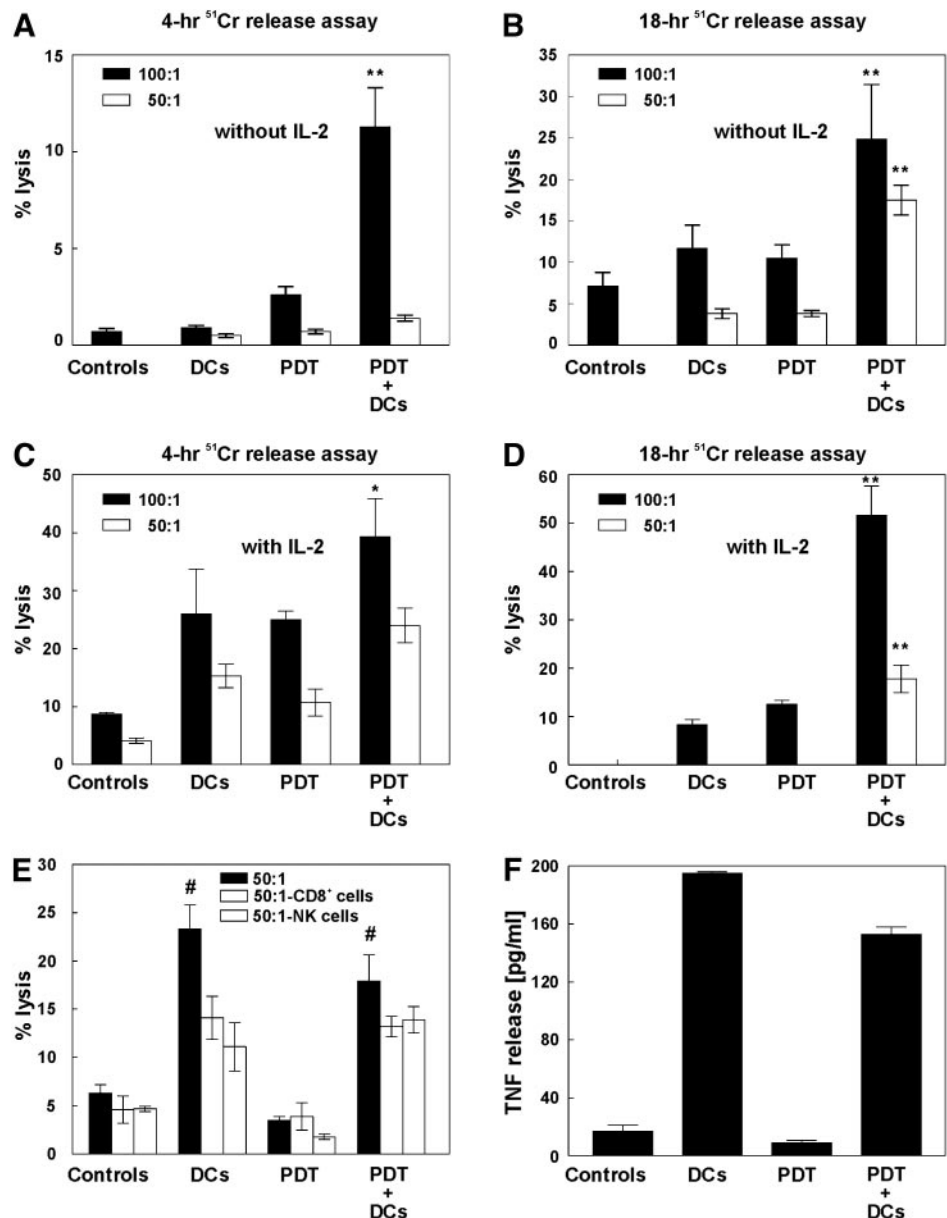
Antitumor Effects of the Combination of PDT and DCs.

To test the concept that administration of DCs after PDT, a treatment that causes necrotic and apoptotic cell death accompanied by oxidative stress and HSP expression can induce an effective antitumor response, we used a transplantable and non-metastasizing C-26 colon adenocarcinoma growing in BALB/c mice. Tumor cells (2×10^5) were inoculated into the right hind limb of experimental animals and were allowed to grow for 7 days before the PDT procedure. On day 6 (one day before laser illumination) mice were given injections of 1×10^5 C-26 cells into the contralateral hind limb. DCs were administered at two doses – 1 h after PDT and 24 h later. This model enabled monitoring of the local growth of PDT-treated tumor (right hind limb) as well as the growth of an unmanipulated tumor (left hind limb) that grows at a distant site, mimicking metastasis. The combination treatment produced the strongest antitumor effects against tumors growing in the right hind limbs (Fig. 5A). The statistical significance ($P < 0.05$; Student's *t* test) was reached on days 16 and 18 after inoculation with C-26 cells. Remarkably strong antitumor effects were also observed in mice treated with the combination of PDT and DCs in the unmanipulated tumors; in six of seven mice, tumors completely disappeared (although the tumors were clearly visible on day 5 after the inoculation with C-26 cells; Fig. 5B).

DISCUSSION

The main finding of this study is that a combination therapy approach using PDT and DCs was more effective than either procedure alone in producing antitumor effects. These observations may have significant translational importance for the development of improved clinical treatment regimens. PDT is a novel treatment modality used for the management of solid tumors and a variety of nonmalignant diseases (1). It is approved for use as a primary therapy for early-stage disease, as a palliation in advanced cancers, and as a surgical adjuvant in the treatment of lung, bladder, esophageal, head and neck, and gastric cancers in many countries. Moreover, PDT is extensively investigated in clinical trials in the treatment of other cancers including breast, colon, and bile duct cancers or brain tumors (1, 3). Likewise, DCs, despite their costly and time-consuming isolation and expansion procedures, are now being examined in several clinical trials. Whereas unmanipulated DCs have shown signs of activity in initial clinical trials, there is an intensive investigation aimed at optimizing their use for therapeutic purposes. Our results strongly support the consideration and devel-

Fig. 4 Cytotoxic activity and tumor necrosis factor (TNF) release from lymph node lymphocytes and spleen cells obtained from mice treated with photodynamic therapy (PDT) and/or dendritic cells (DCs). C-26-bearing mice were treated with PDT (10 mg/kg Photofrin; 90 J/cm² laser light) on day 7 after inoculation with tumor cells. Mice were given injections twice (at 1 h and at 24 h after PDT) with 1 × 10⁶ immature DCs. Seven days later, popliteal lymph nodes and spleen were removed, and cell suspensions were evaluated for cytotoxicity against ⁵¹Cr-labeled C-26 cells. The cytotoxic activity of lymph node lymphocytes was measured in 4-h ⁵¹Cr-release assays (A and C) and 18-h ⁵¹Cr-release assays (B and D). Lymph node lymphocytes were added to ⁵¹Cr-labeled C-26 cells either immediately after isolation from mice (A and B) or after a brief expansion with interleukin 12 (with IL-2; C and D). Spleen cell cytotoxicity was measured in an 18-h ⁵¹Cr-release assay (E) in which spleen cells were incubated with target cells at a ratio of 50:1. Depletion of CD8⁺ T cells (left white columns) and natural killer (NK) cells (right white cells) was performed as described in "Materials and Methods." Additionally, TNF secretion (TNF release) was measured after a 2-day coculture of C-26 cells and spleen cells (F). *, *P* < 0.05 (Student's *t* test) in comparison with all other groups; #, *P* < 0.05 (Student's *t* test) in comparison with controls.



opment of protocols to evaluate the clinical efficacy of combining PDT with DCs.

One of the limitations of PDT is that this treatment modality is effective in the local control of the tumor with very rarely observed and unexplained (presumably immune-mediated) systemic antitumor effects. Therefore, combination strategies that could exploit unique properties of PDT for the induction of systemic antitumor effects are being intensively investigated. PDT induces both necrotic and apoptotic cell death that primarily follow oxidative stress generated by excited photosensitizers. PDT induces rapid and massive release of proinflammatory mediators liberated from cancer cell membranes, damaged endothelial cells, and tumor stroma (26, 27). Moreover, PDT-treated cells secrete a number of cytokines including TNF,

IL-1 β , and IL-6 (28, 29) that participate in the recruitment of neutrophils and other myeloid cells (30). This intense localized inflammation could be appropriately implemented as an initiating event for the induction of effective antitumor immunity. Indeed, a recent study demonstrated that PDT-generated tumor cell lysates are able to activate DCs and can induce antitumor immune response (31); and many studies show strengthened antitumor effectiveness of combinations of PDT with immunomodulators (9, 11).

Tumor cells dying via apoptotic or necrotic mechanisms are a rich source of antigens for processing and presentation by DCs. There are, however, conflicting reports on the immunomodulatory effects exerted by dying tumor cells on the antigen-presenting functions of DCs (32–34). The overwhelming data

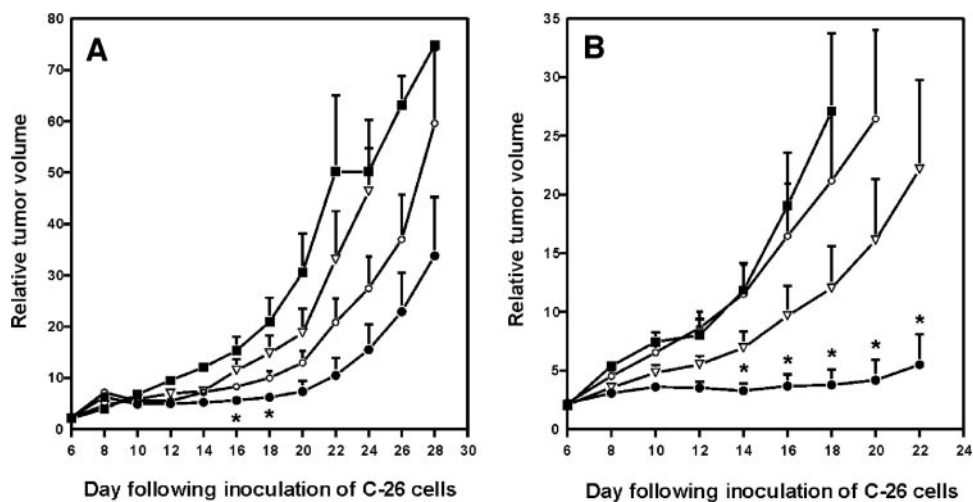


Fig. 5 Antitumor effects of the combined treatment with Photofrin-based photodynamic therapy (PDT) and immature dendritic cells (DCs). ○, PDT; ▽, DCs; ●, PDT+DCs; ■, Controls. Exponentially growing C-26 cells were harvested from cell cultures, resuspended in PBS at a concentration of $2 \times 10^5/20 \mu\text{l}$ of PBS, and injected into the footpad of the right hind limb of experimental mice. Photofrin was administered i.p. at a dose of 10 mg/kg, 24 h before laser illumination (90 J/cm^2 on day 7 after inoculation of tumor cells). DCs (1×10^6) were injected into tumors growing in right hind limbs on days 7 (1 h after PDT) and 8. On day 6 of the experiment, all of the mice were inoculated with 1×10^5 C-26 cells in the left (contralateral) hind limb. Measurements of tumor diameter started on day 6 after inoculation of tumor cells. **A**, the influence of the combined treatment on the growth of C-26 tumors in right hind limbs of BALB/c mice ($n = 7$). **B**, the growth of C-26 tumors in contralateral, untreated hind limbs ($n = 7$). *, $P < 0.05$ (Student's *t* test) in comparison with all other groups.

indicate that apoptotic tumor cells taken up by immature DCs provide antigens in a tolerogenic manner (35). In contrast, *in situ* killing of tumor cells by nonapoptotic mechanisms is associated with high immunogenicity (34). Exposure to heat stress before inducing apoptosis elevates expression of membrane HSPs (HSP72 and HSP60) in apoptotic tumor cells and converts them into more immunogenic cells that are effectively taken up by DCs (17). Inducible HSPs (HSP60, HSP70, and HSP90) activate monocytes and DCs and stimulate the expression of several cytokines such as IL-12 and IL-15 (18, 19), with potent immunoregulatory antitumor activities (36, 37). The immunoregulatory role of other HSPs is less well understood. HSPs chaperone antigenic peptides and channel them into the MHC class I presentation pathway of antigen-presenting cells (38–40). Additionally, some HSPs protect peptides processed by the proteasome from further degradation before being delivered by transporters associated with antigen processing (TAP) proteins to the endoplasmic reticulum for MHC class I loading (40, 41). Finally, down-regulation of HSP70 can lead to inefficient stimulation of the antitumor immune response, and transfection of tumor cell spheroids with HSP70 restores efficient antigen presentation (42). It is unclear how HSPs can stimulate maturation of DCs. Some observations indicate that HSP60 and HSP70 are endogenous stimuli for toll-like receptors that evolved to recognize pathogen-associated molecular patterns of infectious microorganisms (38). The induction of HSP expression may, therefore, provide danger signals required for efficient maturation of DCs.

In our studies, PDT induced significant amounts of several HSPs. Although correlative studies are never fully compelling, it is possible that some HSPs, induced by PDT, function as signature molecules for the activation of DCs maturation and

induction of systemic antitumor response. Several previous studies revealed that stress proteins are expressed after PDT, including HSPs (HSP34, HSP60, HSP70, HSP90, and HSP110) and glucose-regulated proteins [GRPs (GRP74, GRP78, and GRP100); Refs. 43–48]. Some of these proteins are presumed to be involved in rescue responses of cells after PDT (49). Our studies show that these rescue responses might be exploited for more effective tumor treatment. Indeed, coculture of DCs with PDT-treated tumor cells resulted not only in efficient endocytosis of tumor cells but also in a functional activation of antigen-presenting cells that produced a substantial amount of IL-12. Inoculation of immature DCs to the tumors treated with PDT resulted in efficient migration of these cells to both local and distal lymph nodes and stimulation of the cytotoxic activities of lymphocytes isolated from local lymph nodes. The migration of DCs injected into PDT-treated tumors was slightly, but insignificantly, decreased as compared with DCs inoculated into control tumors (Table 1). We can only speculate that this effect is a result of oxidative stress that is induced by the PDT procedure and that leads to decreased viability of injected cells. Moreover, both blood and lymphatic vessels are damaged by PDT, which could contribute to impaired DCs trafficking. Remarkably, the combination treatment leads to the potentiated antitumor response that is not limited to the treated tumor but is also effective in the control of the distant growth. Quite unexpectedly, we observed a stronger antitumor effect of the combination treatment against the tumors inoculated just before PDT into the contralateral footpads. This effect can be explained by the induction of concomitant immunity that is effective in the eradication of small tumor foci but is less efficient in the elimination of larger tumors.

Altogether, intratumorally injected DCs after PDT might prove advantageous in many aspects. Such treatment alleviates the need for the *in vitro* loading with tumor antigens, eliminates concerns regarding unpredictable trafficking of DCs injected via other routes, and allows DCs to acquire, process, and present tumor-derived material in the context of ongoing inflammation, which potentially renders the whole process more immunogenic. Additional studies are definitely necessary to optimize this combination treatment for more effective control of the primary tumor. Our studies are the first report of effective photoimmunotherapy that involves PDT and intratumoral administration of immature DCs. The feasibility of this treatment may warrant additional studies in the clinical setting.

ACKNOWLEDGMENTS

We thank Adam Gołab (Erco Leuchten. GmbH, Warsaw) for the construction of the sodium lamp for *in vitro* experiments, Anna Czerepińska and Elżbieta Gutowska for excellent technical assistance, the Foundation for Polish Science for financing the FACSCalibur, and Dr. Antoni Wrzosek for help with confocal microscopy.

REFERENCES

- Dougherty TJ, Gomer CJ, Henderson BW, et al. Photodynamic therapy. *J Natl Cancer Inst (Bethesda)* 1998;90:889–905.
- Sharman WM, Allen CM, van Lier JE. Role of activated oxygen species in photodynamic therapy. *Methods Enzymol* 2000;319:376–400.
- McBride G. Studies expand potential uses of photodynamic therapy. *J Natl Cancer Inst (Bethesda)* 2002;94:1740–2.
- Henderson BW, Dougherty TJ. How does photodynamic therapy work? *Photochem. Photobiol* 1992;55:145–57.
- Van Duijnhoven FH, Aalbers RI, Rovers JP, Terpstra OT, Kuppen PJ. The immunological consequences of photodynamic treatment of cancer, a literature review. *Immunobiology* 2003;207:105–13.
- Korbelik M, Krosł G, Krosł J, Dougherty GJ. The role of host lymphoid populations in the response of mouse EMT6 tumor to photodynamic therapy. *Cancer Res* 1996;56:5647–52.
- Golab J, Wilczynski G, Zagodzón R, et al. Potentiation of the anti-tumour effects of Photofrin-based photodynamic therapy by localized treatment with G-CSF. *Br J Cancer* 2000;82:1485–91.
- Krosł G, Korbelik M, Krosł J, Dougherty GJ. Potentiation of photodynamic therapy-elicited antitumor response by localized treatment with granulocyte-macrophage colony-stimulating factor. *Cancer Res* 1996;56:3281–6.
- Korbelik M, Sun J. Cancer treatment by photodynamic therapy combined with adoptive immunotherapy using genetically altered natural killer cell line. *Int J Cancer* 2001;93:269–74.
- Krosł G, Korbelik M. Potentiation of photodynamic therapy by immunotherapy: the effect of schizophyllan (SPG). *Cancer Lett* 1994;84:43–9.
- Korbelik M, Cecic I. Enhancement of tumour response to photodynamic therapy by adjuvant mycobacterium cell-wall treatment. *J Photochem Photobiol B* 1998;44:151–8.
- Gomer CJ, Ferrario A, Murphree AL. The effect of localized porphyrin photodynamic therapy on the induction of tumour metastasis. *Br J Cancer* 1987;56:27–32.
- Momma T, Hamblin MR, Wu HC, Hasan T. Photodynamic therapy of orthotopic prostate cancer with benzoporphyrin derivative: local control and distant metastasis. *Cancer Res* 1998;58:5425–31.
- Guermontprez P, Valladeau J, Zitvogel L, Thery C, Amigorena S. Antigen presentation and T cell stimulation by dendritic cells. *Annu Rev Immunol* 2002;20:621–67.
- Larsson M, Fonteneau JF, Bhardwaj N. Dendritic cells resurrect antigens from dead cells. *Trends Immunol* 2001;22:141–8.
- Gallucci S, Matzinger P. Danger signals: SOS to the immune system. *Curr Opin Immunol* 2001;13:114–9.
- Feng H, Zeng Y, Whitesell L, Katsanis E. Stressed apoptotic tumor cells express heat shock proteins and elicit tumor-specific immunity. *Blood* 2001;97:3505–12.
- Flohe SB, Bruggemann J, Lendemans S, et al. Human heat shock protein 60 induces maturation of dendritic cells versus a Th1-promoting phenotype. *J Immunol* 2003;170:2340–8.
- Chen W, Syldath U, Bellmann K, Burkart V, Kolb H. Human 60-kDa heat-shock protein: a danger signal to the innate immune system. *J Immunol* 1999;162:3212–9.
- Inaba K, Inaba M, Romani N, et al. Generation of large numbers of dendritic cells from mouse bone marrow cultures supplemented with granulocyte/macrophage colony-stimulating factor. *J Exp Med* 1992;176:1693–702.
- Jalili A, Stokłosa T, Giermasz A, et al. A single injection of immature dendritic cells is able to induce antitumor response against a murine colon adenocarcinoma with a low apoptotic index. *Oncol Rep* 2002;9:991–4.
- Kozar K, Kaminski R, Switaj T, et al. Interleukin 12-based immunotherapy improves the antitumor effectiveness of a low-dose 5-aza-2'-deoxycytidine treatment in L1210 leukemia and B16F10 melanoma models in mice. *Clin Cancer Res* 2003;9:3124–33.
- Golab J, Nowis D, Skrzycki M, et al. Antitumor effects of photodynamic therapy are potentiated by 2-methoxyestradiol. A superoxide dismutase inhibitor. *J Biol Chem* 2003;278:407–14.
- Golab J, Stokłosa T, Zagodzón R, et al. G-CSF prevents the suppression of bone marrow hematopoiesis induced by IL-12 and augments its antitumor activity in a melanoma model in mice. *Ann Oncol* 1998;9:63–9.
- Porgador A, Snyder D, Gilboa E. Induction of antitumor immunity using bone marrow-generated dendritic cells. *J Immunol* 1996;156:2918–26.
- Agarwal ML, Larkin HE, Zaidi SI, Mukhtar H, Oleinick NL. Phospholipase activation triggers apoptosis in photosensitized mouse lymphoma cells. *Cancer Res* 1993;53:5897–902.
- Henderson BW, Donovan JM. Release of prostaglandin E2 from cells by photodynamic treatment *in vitro*. *Cancer Res* 1989;49:6896–900.
- Gollnick SO, Liu X, Owczarczak B, Musser DA, Henderson BW. Altered expression of interleukin 6 and interleukin 10 as a result of photodynamic therapy *in vivo*. *Cancer Res* 1997;57:3904–9.
- Nseyo UO, Whalen RK, Duncan MR, Berman B, Lundahl SL. Urinary cytokines following photodynamic therapy for bladder cancer. A preliminary report. *Urology* 1990;36:167–71.
- Gollnick SO, Evans SS, Baumann H, et al. Role of cytokines in photodynamic therapy-induced local and systemic inflammation. *Br J Cancer* 2003;88:1772–9.
- Gollnick SO, Vaughan L, Henderson BW. Generation of effective antitumor vaccines using photodynamic therapy. *Cancer Res* 2002;62:1604–8.
- Jenne L, Arrighi JF, Jonuleit H, Saurat JH, Hauser C. Dendritic cells containing apoptotic melanoma cells prime human CD8+ T cells for efficient tumor cell lysis. *Cancer Res* 2000;60:4446–52.
- Kotera Y, Shimizu K, Mule JJ. Comparative analysis of necrotic and apoptotic tumor cells as a source of antigen(s) in dendritic cell-based immunization. *Cancer Res* 2001;61:8105–9.
- Sauter B, Albert ML, Francisco L, Larsson M, Somersan S, Bhardwaj N. Consequences of cell death: exposure to necrotic tumor cells, but not primary tissue cells or apoptotic cells, induces the maturation of immunostimulatory dendritic cells. *J Exp Med* 2000;191:423–34.
- Steinman RM, Hawiger D, Nussenzweig MC. Tolerogenic dendritic cells. *Annu Rev Immunol* 2003;21:685–711.
- Fehniger TA, Cooper MA, Caligiuri MA. Interleukin-2 and interleukin-15: immunotherapy for cancer. *Cytokine Growth Factor Rev* 2002;13:169–83.

37. Golab J, Zagozdzon R. Antitumor effects of interleukin-12 in pre-clinical and early clinical studies [Review]. *Int J Mol Med* 1999;3: 537–44.
38. Dangles-Marie V, Richon S, El-Behi M, et al. A three-dimensional tumor cell defect in activating autologous CTLs is associated with inefficient antigen presentation correlated with heat shock protein-70 down-regulation. *Cancer Res* 2003;63:3682–7.
39. Vabulas RM, Ahmad-Nejad P, Ghose S, Kirschning CJ, Issels RD, Wagner H. HSP70 as endogenous stimulus of the Toll/interleukin-1 receptor signal pathway. *J Biol Chem* 2002;277:15107–12.
40. Binder RJ, Blachere NE, Srivastava PK. Heat shock protein-chaperoned peptides but not free peptides introduced into the cytosol are presented efficiently by major histocompatibility complex I molecules. *J Biol Chem* 2001;276:17163–71.
41. Castellino F, Boucher PE, Eichelberg K, et al. Receptor-mediated uptake of antigen/heat shock protein complexes results in major histocompatibility complex class I antigen presentation via two distinct processing pathways. *J Exp Med* 2000;191:1957–64.
42. Srivastava PK, Udono H, Blachere NE, Li Z. Heat shock proteins transfer peptides during antigen processing and CTL priming. *Immunogenetics* 1994;39:93–8.
43. Gomer CJ, Ryter SW, Ferrario A, Rucker N, Wong S, Fisher AM. Photodynamic therapy-mediated oxidative stress can induce expression of heat shock proteins. *Cancer Res* 1996;56:2355–60.
44. Gomer CJ, Ferrario A, Rucker N, Wong S, Lee AS. Glucose regulated protein induction and cellular resistance to oxidative stress mediated by porphyrin photosensitization. *Cancer Res* 1991;51: 6574–9.
45. Gomer CJ, Luna M, Ferrario A, Rucker N. Increased transcription and translation of heme oxygenase in Chinese hamster fibroblasts following photodynamic stress or Photofrin II incubation. *Photochem Photobiol* 1991;53:275–9.
46. Curry PM, Levy JG. Stress protein expression in murine tumor cells following photodynamic therapy with benzoporphyrin derivative. *Photochem Photobiol* 1993;58:374–9.
47. Hanlon JG, Adams K, Rainbow AJ, Gupta RS, Singh G. Induction of Hsp60 by Photofrin-mediated photodynamic therapy. *J Photochem Photobiol B* 2001;64:55–61.
48. Wang HP, Hanlon JG, Rainbow AJ, Espiritu M, Singh G. Up-regulation of Hsp27 plays a role in the resistance of human colon carcinoma HT29 cells to photooxidative stress. *Photochem Photobiol* 2002;76:98–104.
49. Moor AC. Signaling pathways in cell death and survival after photodynamic therapy. *J Photochem Photobiol B* 2000;57:1–13.